Unconventional magnetism in all-carbon nanofoam

A. V. Rode,[1,*,†] E. G. Gamaly,[1] A. G. Christy,[2] J. G. Fitz Gerald,[3] S. T. Hyde,[1] R. G. Elliman,[1] B. Luther-Davies,[1] A. I. Veinger,[4] J. Androulakis,[5] and J. Giapintzakis[5,6,*,‡]

[1]*Research School of Physical Sciences and Engineering, Australian National University, Canberra, ACT 0200, Australia*

[2]*Department of Earth and Marine Science, Australian National University, Canberra, ACT 0200, Australia*

[3]*Research School of Earth Sciences, Australian National University, Canberra, ACT 0200, Australia*

[4]*Ioffe Physical-Technical Institute, Polytechnicheskaya 26, St. Petersburg, Russia*

[5]*Foundation for Research and Technology-Hellas, Institute of Electronic Structure and Lasers, P.O. Box 1527, Vasilika Vouton, 71110 Heraklion, Crete, Greece*

[6]*Department of Materials Science and Technology, University of Crete, P.O. Box 2208, 710 03 Heraklion, Crete, Greece*

(Received 11 September 2003; revised manuscript received 28 May 2004; published 17 August 2004)

We report production of nanostructured magnetic carbon foam by a high-repetition-rate, high-power laser ablation of glassy carbon in Ar atmosphere. A combination of characterization techniques revealed that the system contains both sp^2 and sp^3 bonded carbon atoms. The material is a form of carbon containing graphite-like sheets with hyperbolic curvature, as proposed for "schwarzite." The foam exhibits ferromagnetic-like behavior up to 90 K, with a narrow hysteresis curve and a high saturation magnetization. Such magnetic properties are very unusual for a carbon allotrope. Detailed analysis excludes impurities as the origin of the magnetic signal. We postulate that localized unpaired spins occur because of topological and bonding defects associated with the sheet curvature, and that these spins are stabilized due to the steric protection offered by the convoluted sheets.

DOI: 10.1103/PhysRevB.70.054407 PACS number(s): 75.75.+a, 78.67.Bf, 81.15.Fg, 61.46.+w

I. INTRODUCTION

The materials science of carbon has proven to be a rich area of discovery and development in the past decades. Until relatively recently, the only known polymorphs of carbon were graphite, in which sp^2 hybridized carbon atoms form planar sheets in a two-layer hexagonal stacking, and diamond, in which sp^3 carbons form a three-dimensional framework of cubic symmetry. However, in recent years new carbon allotropes have proliferated. A three-layer rhombohedral stacking modification of graphite was reported in 1956[1] and lonsdaleite, the two-layer hexagonal polytype of diamond, was discovered in shocked rocks in a meteorite crater in 1967.[2] Fibrous sp^1-hybridized carbon has been identified in a mineral environment;[3] similar "carbynes" have been suggested to occur in interstellar dust,[4] and similar materials have been synthesized by shock compression of graphite.[5–9] A broad spectrum of "turbostratic graphites" are also known, in which individual graphene layers show rotational and tilt disorder relative to their neighbors. A recent extreme example is provided by cores of carbon spherules in the Murchison meteorite, which are aggregates of randomly oriented single layers with additional structure defects.[10] This particular specimen is among the oldest known naturally occurring material, since it solidified before the condensation of the Solar System. In contrast, recently synthesized materials include many further distinct forms of carbon such as fullerenes,[11,12] multiwalled carbon nanotubes,[13] and single-walled carbon nanotubes,[14] which are based on a mixture of sp^2 and sp^3 hybridized carbon atoms. The structural phase space of carbon between graphite-like and diamond-like hybridization states now has many occupants. There is even more variety in the electronic properties of various carbon allotropes, which range from superconductivity[15] to ferromagnetism[16] and tunable electrical conductivity.[17–19] Such effects have attracted enormous attention and already been proposed for commercial applications.[20]

A physical property of particular interest regarding all the aforementioned carbon allotropes is the magnetic susceptibility, χ, since this bulk probe is related to the low energy electronic spectrum. In general, all known carbon allotropes exhibit diamagnetic susceptibility in the range of $\chi = -(10^{-5}-10^{-7})$ emu/g Oe with the exception of: (i) polymerized C_{60} prepared in a two-dimensional rhombohedral phase of $\chi = +(0.25-1.3)\times 10^{-3}$ emu/g Oe (depending on the orientation of the magnetic field relative to the polymerized planes) which shows ferromagnetism;[16] (ii) the disordered glass-like magnetism observed in activated carbon fibers due to nonbonding π electrons located at edge states;[21] and (iii) the unusual magnetic behavior observed in single wall carbon nanohorns ascribed to the Van Vleck paramagnetic contribution.[22] Although ferromagnetism in polymerized C_{60} is noteworthy, the exceptionally large magnetic signal in carbon nanostructures remains a case of special interest.[23]

Superparamagnetic and/or ferromagnetic-like behavior in carbon-based material has been previously observed in amorphous carbon materials obtained by chemical synthesis or pyrolysis.[24,25] The origin of ferromagnetism was suggested to be attributed to the mixture of carbon atoms with sp^2 and sp^3 bonds and resulted ferromagnetic interaction of spins separated by sp^3 centers.[26] An increase in saturated magnetization of amorphous-like carbon prepared from different hydrogen-rich materials indicated the importance of hydrogen in the formation of the magnetic ordering in graphite.[27,28] Very recently, ferro- or ferrimagnetic ordering was discovered in proton-irradiated spots in highly oriented

pyrolytic graphite (HOPG).[29] It was demonstrated that protons implanted in HOPG triggered ferro- (or, ferri-) magnetic ordering with a Curie temperature above room temperature. To check the importance of hydrogen, spots of similar topography were produced with helium ion irradiation. Those spots showed no significant magnetic signal in magnetic force microscopy measurements, which stressed the significance of hydrogen in the formation of magnetic ordering in graphite. These findings were supported by theoretical predictions,[30] which show that hydrogenated graphite can display spontaneous magnetization originating from different numbers of mono- and double-hydrogenated carbon atoms.

We have recently synthesized a new form of carbon: cluster-assembled carbon nanofoam, by laser ablation of glassy carbon in an argon-filled chamber using a high-repetition rate high-power laser.[31–33] The synthesis technique is to our knowledge unique. We characterized the carbon nanofoam by several electron microscopy techniques, which revealed a web-like structure containing randomly interconnected clusters, 4–9 nm in diameter. The nanofoam exhibits some remarkable physical properties, including ultralow density ($\sim 2-10$ mg/cm^3, the lowest gravimetric density ever reported for a solid), and a large surface area (comparable to zeolites) of 300–400 m^2/g.[31,32]

Here we report the equally unusual magnetic properties of the cluster-assembled nanofoam. The foam shows strong positive magnetization, some of which is lost in the first few hours after synthesis, but much of which is persistent. This paper presents a detailed study of one sample, which displayed a saturation magnetization of $M_s = +0.42$ emu/g at 1.8 K 12 months after synthesis. We assess and eliminate impurities as significant contributors to the measured properties and conclude that the observed behavior, which can neither be ascribed to paramagnetism nor to conventional soft/weak ferromagnetism, is an intrinsic property of the nanofoam.

According to the theoretical predictions,[34–37] hypothetical hyperbolic carbon structures (with negative Gaussian curvature), branded as "schwarzites," exhibit complex bonding and electronic structure relative to fullerenes (elliptic curvature) and buckytubes (parabolic curvature). It has been suggested that the spatial structure of schwarzites might result in unusual electronic properties. High-resolution transmission electron micrographs (HRTEM) of the nanofoam revealed patterns characteristic of hyperbolically curved graphitic sheets. We therefore consider the presence of schwarzite structure as a possible origin for ferromagnetic interaction of unpaired spins in the hydrogen-free carbon nanofoam.

II. EXPERIMENTAL DETAILS

A. Synthesis

The low-density cluster-assembled carbon nanofoam was produced by high-repetition-rate (2–25 kHz) laser ablation of an ultrapure glassy carbon target in a vacuum chamber made of stainless steel with the base vacuum $\sim 5 \times 10^{-7}$ Torr, filled with high-purity (99.995%) Ar gas, inside a 2 in. cylinder made of fused silica (SiO_2). The deposited foam was scraped off from the inner cylinder surface with plastic tweezers and placed into a glass vial for further analysis. Full details regarding the experimental conditions can be found elsewhere.[31–33] Here, we briefly explain some unique features of the synthesis conditions, which are different from any previously used nanocluster synthesis method.

The carbon vapor temperature in the laser plume, where the formation process takes place, is in the range 1–10 eV (10 000–100 000 K), i.e., the formation takes place in a partly ionized plasma.[38] The high-repetition-rate laser ablation creates an almost continuous inflow of hot carbon atoms and ions with an average temperature of ~ 2 eV into the experimental chamber. This vapor heats the ambient gas and increases the partial density of carbon atoms in the chamber. The process of formation of carbonaceous clusters begins when the carbon density reaches the threshold density, at which the probability of collisions between carbon atoms becomes sufficiently high.

The consumption rate of carbon atoms due to the cluster formation significantly exceeds the evaporation rate by laser ablation in the experimental conditions of high-repetition-rate laser ablation.[32,38] Thus, the formation is a nonequilibrium periodical process. We suggest that the formation process comprises periodic heating and cluster formation stages, with the time period dependent on the initial Ar density, the evaporation rate, and reaction rate, which in turn is a function of the temperature and density of the atomic carbon. It is essential that during the period of cluster formation, short in comparison to the heating period, the argon gas does not cool down, but maintains its high temperature for cluster formation. Hence, the argon (and carbon vapor) temperature from the second formation cycle onward is higher than the formation threshold temperature, which is believed to initiate sp^2 bonding. The still higher temperature achieved during subsequent cycles is sufficient to form sp^3 bonds along with the sp^2 bonds observed in the cluster-assembled carbon foam.

B. Characterization

In order to check the reproducibility of our results we have produced several samples. Structural and electronic properties of the samples were characterized by means of scanning electron microscopy (SEM), HRTEM, electron energy loss spectroscopy, Rutherford back-scattering (RBS), heavy ion elastic recoil detection (ERD), electron spin resonance measurements (ESR), and trace elemental analysis by induction-coupled plasma mass spectrometry (ICP-MS) of acid extracts.

It was already evident from the first samples of the foam that the material displays interesting electronic properties. The as-deposited samples had a strong positive electrostatic charge; indeed, the charge was so high that considerable difficulty was encountered in placing the foam into a glass vial. This behavior implied at once that the dielectric properties of the carbon nanofoam are different from those of carbon aerogels and other carbon nanometer-size porous structures.[39–41] This difference can be attributed to the formation conditions: the foam clusters are formed in a very high temperature environment of partially ionized carbon plasma.[38] The carbon nanofoam has a significant $sp^3/(sp^2+sp^3)$ bonding ratio of

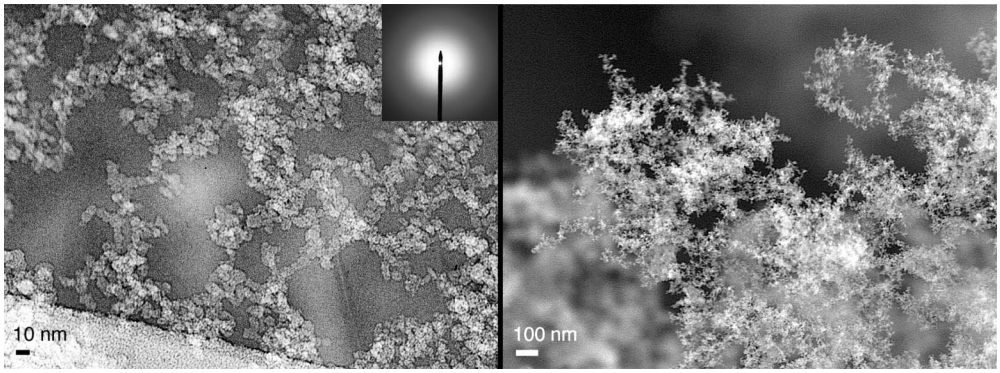

FIG. 1. Transmission electron micrograph (left), and scanning electron micrograph (right) of the carbon nanofoam, showing the web-like structure. The diffraction pattern in the inset shows the very broad rings indicating the lack of a long-range three-dimensional order in the foam.

35% on average, and up to 60% in some regions. The spatial variation of $sp^3/(sp^2+sp^3)$ bonding across individual clusters was mapped using the parallel electron energy loss spectrometer (PEELS) with a spatial resolution of 1 nm. The analysis indicates that sp^2 bonded carbons prevail in the core, whereas sp^3 bonded carbons prevail near the cluster boundary and bond the clusters together.[31] The ERD analysis with 200 MeV Au ions did not show the presence of hydrogen in the foam, at least at the sensitivity level of 0.1% atomic.

The electrical direct current conductivity of amorphous carbon (*a*-C) is strongly dependent on the sp^3 content, falling by over eight orders of magnitude as the sp^3 fraction increases.[42] The conductivity of the nanofoam increases from $\sim(2-5)\times10^{-13}$ S cm^{-1} at 85 K to 3×10^{-10} S cm^{-1} at room temperature, and to $\sim10^{-8}$ S cm^{-1} at 400 K, exhibiting semiconducting behavior. The conductivity measurements are consistent with our observation that sp^2 regions are separated by surrounding sp^3 carbon atoms. Optical transmission spectral measurements show that the nanofoam has a narrow fundamental band gap in the range of 0.5–0.7 eV,[31] which is typical for a hydrogen-free diamond-like amorphous carbon.

ESR analysis shows a single, wide line, with g factor and the half-width parameters of $g=2.0025, \Delta H=7.5$ Oe at 300 K and $\Delta H=2$ Oe at 77 K.[32] We measured the spin density of the carbon nanofoam of 1.8×10^{20} spins per gram of foam mass in average. This corresponds to approximately one unpaired spin per $\sim$300 carbon atoms. The nanofoam has the highest spin density reported for a three-dimensional pure carbon solid, although we note that similarly high spin densities have been reported for sp^3-rich amorphous carbon as thin films.[40,42]

C. Nanostructure

Low-resolution TEM images clearly show the presence of small randomly interconnected clusters with the diameters in the range from 4 to 9 nm, with the average size of 6.1 nm (Fig. 1).

Our structural studies revealed the presence of hyperbolic schwarzite structures.[31,33] Schwarzites are anticlastic (saddle-shaped) warped graphite-like layers, in contrast to the synclastic sheets characteristic of fullerenes.[34] Fourier transforms and subsequent radial regrouping of the HRTEM micrographs ($\times1\,000\,000$) indicated the existence of a structural period in the clusters with a space scale of 5.6 ± 0.4 Å (see Fig. 2).[31] This "repeat" spacing is not due to smectic layering within the carbon structure, as Fourier transforms of the TEM images collected from the smallest possible domains (about 100×100 Å) reveal a spatially isotropic "powder"-like diffraction ring. The number of carbon atoms per cluster was estimated to be $\sim1.2\times10^4$ (molecular weight 1.38×10^5). This leads to a cluster density of 1.95 g/cm^3. A value of similar order of magnitude 1.65 g/cm^3 was derived from the results of mapping of individual clusters by a 1 nm electron beam in PEELS.[31]

D. Chemical impurities

The possibility of magnetic contamination during synthesis of the nanofoam samples was examined in some detail, as this would offer a simple explanation for the peculiar magnetic features of the material. The impurity content in the foam was determined from 2 MeV He^+ ion RBS measurements, and independently by mass spectroscopy analysis of acid extracts from the foam. Both methods show comparable low impurity contents. The RBS data indicated a total concentration of Fe-Ni below 100 ppm atomic. Mass spectrometry measurements were done on milligram samples of the foam, extracted with concentrated HCl for several hours, diluted with 2% HNO_3, filtered and run in a Varian Ultramass quadrupole spectrometer. Initially, three separately synthesized samples of foam were analyzed for the elements Al, Ti, V, Cr, Co, Ni, Cu, Sn, and Pb. One sample, selected to be the subject of the current magnetization study, had a second portion analyzed for an extended list of elements that included Sc, Mn, Fe, Zn, Ga, In, Sb, and Bi (Table I), although we note that the molecular species ArO interferes strongly with Fe and produces a false high signal at the Fe mass numbers. The sum of all the impurity elements analyzed in the foam of this study was 415–465 ppm assuming 30 ppm (the Ni concentration) $<$Fe$<$80 ppm. The dominant impurity elements in the samples were Al, Cu, Zn, Pb, Ni, and probably Fe. The elemental makeup, in combination

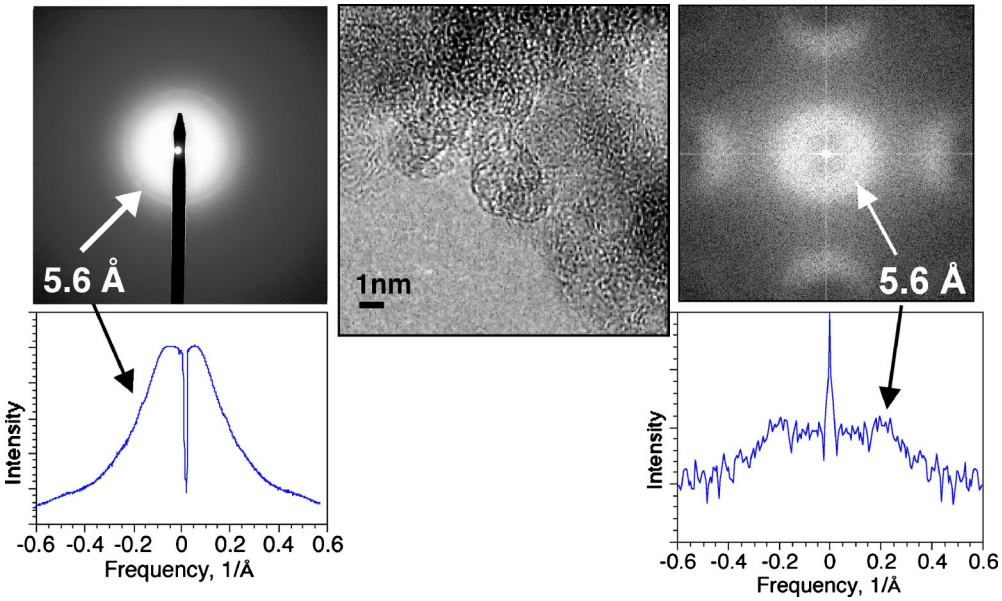

FIG. 2. High-resolution TEM image of the carbon nanofoam foam (central image) with an individual 6 nm cluster clearly seen in the center. Fourier transforms (right) and electron diffraction patterns (left) indicate a "repeat" spacing with characteristic length of 5.6±0.4 Å typical for schwarzites.

with considerable run-to-run variability of impurity content are compatible with the hypothesis that the impurities are introduced randomly as metallic dust particles (primarily aluminum, brass, solder, and stainless steel) originating in the apparatus. SEM examination of one of the ablation targets did in fact reveal scattered micron-scale particles of aluminum metal, lending further support to this hypothesis.

TABLE I. Trace element analysis (ICP-MS) of carbon foam samples. Fe determination is a maximum value due to $^{40}Ar^{17}O$ interference at same mass number. Stated uncertainties are standard deviations for five replicate measurements as an indication of spectrometer reproducibility.

Element	Atomic ppm
Al	125±4
Sc	0.5±0.3
Ti	0.4±7
V	0.2±4
Cr	11±1
Mn	5.5±0.3
Fe	<80
Co	0.65±0.07
Ni	29.7±1.5
Cu	110±7
Zn	67±5
Ga	0.4±0.2
In	0.12±0.02
Sn	5.6±0.5
Sb	0.19±0.09
Pb	24±1
Bi	3.8±0.2

E. Magnetization measurements

All magnetization measurements were performed in a commercial extraction magnetometer (Maglab Exa 2000) by Oxford Instruments in the temperature range $1.8 \leqslant T \leqslant 300$ K and in applied magnetic fields up to 70 kOe. Reproducibility of the magnetic properties of the foam is demonstrated by the comparable magnetization (0.36–0.8 emu/g) measured in six independently synthesized batches of foam 15 days after synthesis (Table II). The magnetization of the foam in this study (0.42 emu/g at 60 days and 12 months after the synthesis) is evidently typical for the material.

The nanofoam magnetic response to temperature and applied field were investigated in detail. Figure 3 presents the temperature dependence of the mass magnetization (closed circles) of the carbon nanofoam measured at 30 kOe in the temperature range $1.8 \leqslant T \leqslant 200$ K. The curve has been corrected for the diamagnetic background of the gelatine sample holder, which was measured independently under the same conditions (crosses in Fig. 3). The raw data of the composite (carbon nanofoam + sample holder) are represented by the

TABLE II. Magnetization measurements of carbon foam samples 15 days after synthesis. Magnetization measured at $T = 5$ K, $H = 60$ kOe.

Sample	Magnetic condition	Mass magnetization (emu/g)
040602	Paramagnetic	0.446
050602#1	Paramagnetic	0.366
050602#2	Paramagnetic	0.8
060602#1	Paramagnetic	0.375
060602#2	Paramagnetic	0.78
070602	Paramagnetic	0.5

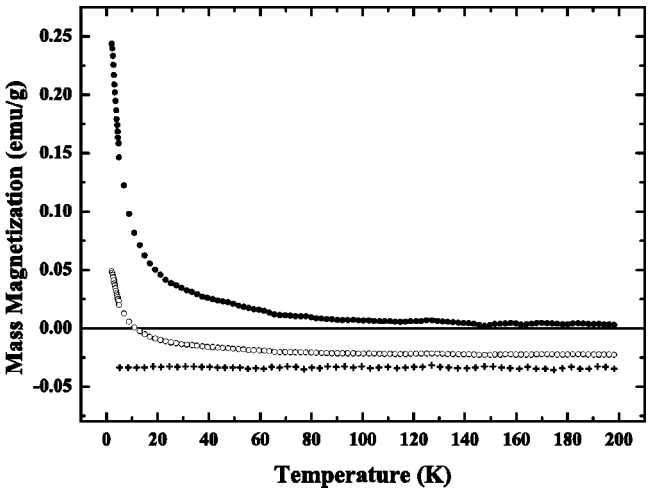

FIG. 3. Temperature dependence of the mass magnetization of the composite of carbon nanofoam and sample holder (open circles), the carbon nanofoam (filled circles), and the gelatine sample holder (crosses) measured at 30 kOe in the temperature range $1.8 \leqslant T \leqslant 200$ K.

open circles in Fig. 3. All data were collected following zero-field cooling of the sample at a heating rate of 0.3 K/min. The observed signal is positive and apparently paramagnetic (PM). However, the expected PM $1/T$-dependence was not observed, which is indicative of a non-Curie-Weiss system. Hence, magnetization isotherms at low temperatures were investigated.

Figure 4 illustrates the mass magnetization of the foam as a function of the applied magnetic field at several temperatures from 1.8 to 92 K. All data have been corrected for the diamagnetic contribution of the gelatine sample holder that was again measured separately under the same conditions. The measured signal is positive and the curves show PM-like behavior. Nevertheless, we observe a slight hysteresis with a

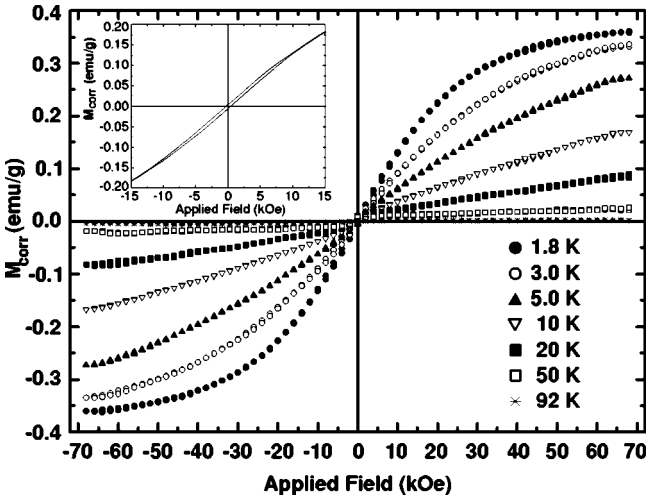

FIG. 4. Mass magnetization of the foam as a function of the applied magnetic field, $M(H)$, at several temperatures from 1.8 to 92 K. All data are corrected for the diamagnetic contribution of the gelatine sample holder. Inset: $M(H)$, hysteresis loop at $T=1.8$ K exhibiting a coercive force $H_c=420$ Oe.

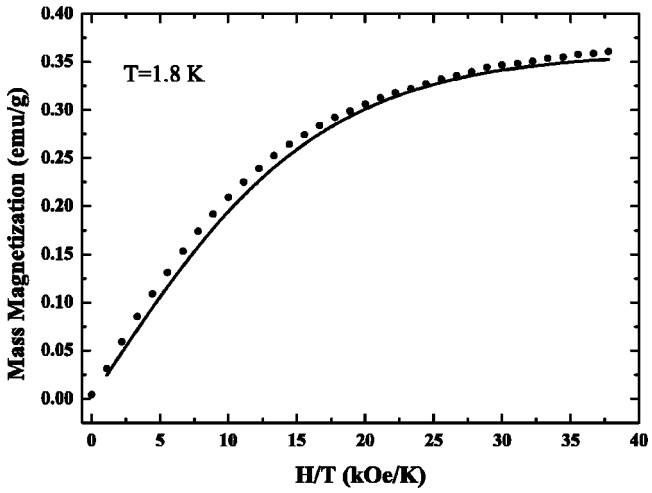

FIG. 5. Corrected mass magnetization of the foam as a function of H/T measured at $T=1.8$ K. Solid line is a fit of the data to the Brillouin function with $S=1/2$.

well-defined coercive force at low temperatures (see inset of Fig. 4) as expected for a ferromagnet (FM). In Fig. 5 we present the first quadrant of the magnetization isotherm taken at 1.8 K. The open circles are the magnetization data, while the solid line represents a fit of the measured magnetization values to the Brillouin function with $S=1/2$, which corresponds only roughly to the observed behavior.

$M(H)$ data taken at $T=1.8$ K, were plotted against $1/H$ in order to obtain the saturation magnetization of 0.42 emu/g after extrapolation to infinite field. This is equivalent to a saturation moment value of $9.0\times10^{-4}\mu_B$ per carbon atom (μ_B is the Bohr magneton equal to 9.27×10^{-21} erg/G). Assuming that our spin system is FM-like rather than PM (i.e., $1\mu_B$ per unpaired spin), we estimate that this value corresponds to about 1 unpaired spin per 1000 carbon atoms, a fact which suggests that several unpaired spins are located in each of the nanometer-scale spheroidal clusters with $\sim10^4$ C atoms/cluster that constitute the foam,[31] and is in order-of-magnitude agreement with low temperature ESR measurements that show a large concentration of unpaired spins 1.8×10^{20}/g (3.6 unpaired spins per 1000 carbon atoms).

III. DISCUSSION OF MAGNETIZATION DATA

We have observed a strong positive magnetization signal in an all-carbon structure, which seems to have features of both a PM and a FM. It could be hypothesized that our observed sample behavior combines a FM signal from chemical impurities (the 3*d* elements) and PM from the carbon phase (foam). However, the experimental evidence does not support this possibility. We now show that the observed magnetic behavior cannot arise from ferromagnetic impurities but rather is an intrinsic property of the nanofoam.

First, consider the magnitude of the observed signal. Both the hysteretic behavior as well as the relative failure of the Brillouin model might be attributable to the existence of FM impurities (see Table I). Nonlanthanide FM compounds have

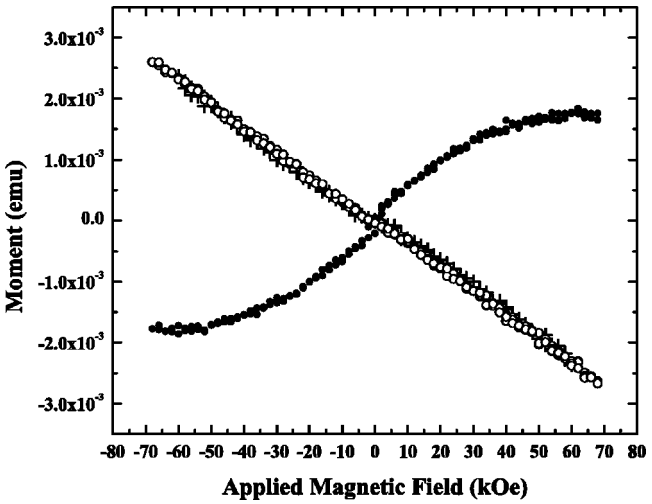

FIG. 6. Magnetic moment as a function of the applied magnetic field for the gelatin sample holder measured at $T=5$ K (crosses), and the composite of carbon nanofoam and sample holder measured at $T=5$ K (closed circles) and $T=110$ K (open circles).

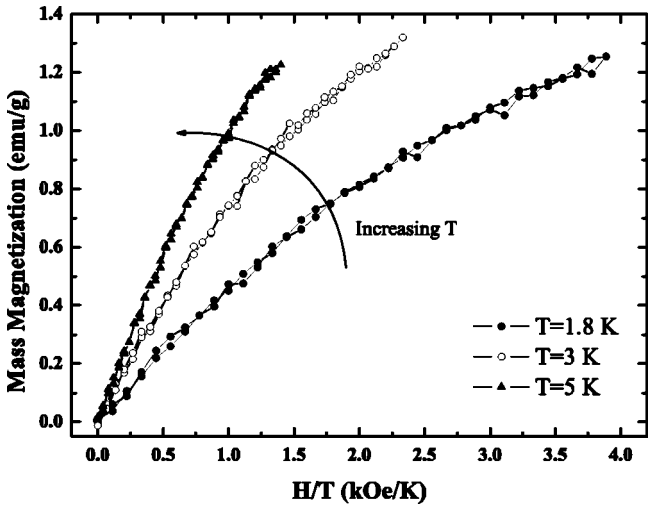

FIG. 7. Corrected mass magnetization as a function of H/T at $T=1.8$ K (closed circles), 3 K (open circles), and 5 K (triangles). Note that the curves do not scale as it is expected for a PM and have the opposite behavior from that expected for a FM.

saturation magnetizations corresponding to effective Bohr magneton numbers of $0.5-3.5\mu_B$ per magnetic atom.[43] If we assume an absolute worst-case scenario in which all the Fe, Co, and Ni were in their ferromagnetic elemental forms, the impurity magnetization would be at most 0.09 emu/g in our sample, which is only 20% of the measured total. We note that even Fe-Ni are likely to be present as non-FM steel. The 3*d* elements Sc-Cu make up only half of the impurity total, and the elements Fe-Ni are less than half again of that fraction. Many of the impurity elements are most likely to be present in nonferromagnetic phases such as Al metal, brass, and solder.

Furthermore, the observed response of sample magnetism to temperature and applied magnetic field is not what would be expected from transition metal bearing ferromagnetic impurities. A ferromagnetic contribution from impurity elements should remain constant (saturated) at a specific temperature for sufficiently high magnetic field values (a few kilo-oersted for normal FM elements) and should also change only slightly with temperature given the fact that normal 3*d*-FM elements exhibit a critical Curie temperature T_c of the order of ~ 1000 K ($T_c=1043, 1388$, and 627 K for Fe, Co, and Ni metals, respectively), as do many of their intermetallic compounds with B-group semimetals (e.g., MnBi, $T_c=630$ K; Cu_2MnAl, $T_c=710$ K).[43]

Because of the relative temperature insensitivity, we would expect an "impurity" signal to persist at high temperatures. However, the magnetism of our sample does not behave in that way, as is evident from Fig. 6, where we have plotted the total measured signal of the composite (foam + gelatine holder) at $T=5$ K and $T=110$ K as well as the measured signal of the sample holder alone as a function of the applied magnetic field. If the total measured signal was predominantly due to FM impurities, then the same pattern should have been observed at quite elevated temperatures. Nevertheless, above ~ 100 K the remaining signal from the composite is comprised almost entirely of the nearly temperature-independent diamagnetic signal of the gelatine sample holder. The open circles represent a M vs H measurement at $T=5$ K of the gelatine sample holder and is plotted for clarity on the same graph (Fig. 6). The strong applied field dependence of the total signal is clear. These data indicate that the observed magnetic behavior is extremely unlikely to arise from ferromagnetic impurities.

We now turn to the "PM"-like signal of Figs. 4 and 5. It is well known that the magnetization of a PM, when plotted against normalized H/T for several different temperatures, should collapse onto a single curve. Figure 7 shows a plot of the magnetization of the foam versus H/T. Data for different T do not scale similarly, a clear indication that the sample is not simply paramagnetic (or superparamagnetic). Although, the "FM-impurities" argument could account for such an effect, this conclusion is contra-indicated by the observation that the magnetization is higher at higher temperatures, i.e., the $M(H/T)$ curve at 5 K is above that of the curve extracted at 3 K. The same is true for the curve at 3 K and so on. If the magnetization were dominated by "impurity" FM interactions then the situation would be reversed. A similar effect to that in our sample has recently been observed in amorphous magnetic rare earth silicon alloys[44] where the formation of ferromagnetic polarons where found to play a crucial role. The authors of Ref. 44 have speculated that competition of intrapolaron FM interactions and interpolaron antiferromagnetic interactions due to significant polaron overlapping can explain their data.

Another possible source of positive susceptibility is molecular oxygen. Molecular oxygen—one of the most abundant nonmetallic paramagnets in nature—is a possible source of contamination since it can potentially be trapped as an adsorbate on a high surface area material such as our foam. However, intercalation into the 5–6 Å gaps between sheets is unlikely, since the sum of two carbon Van der Waals radii (1.7 Å each) and two oxygen radii (1.5 Å each) is 6.4 Å. We note that the data reported in the current study were collected from samples that were handled in pure helium atmosphere

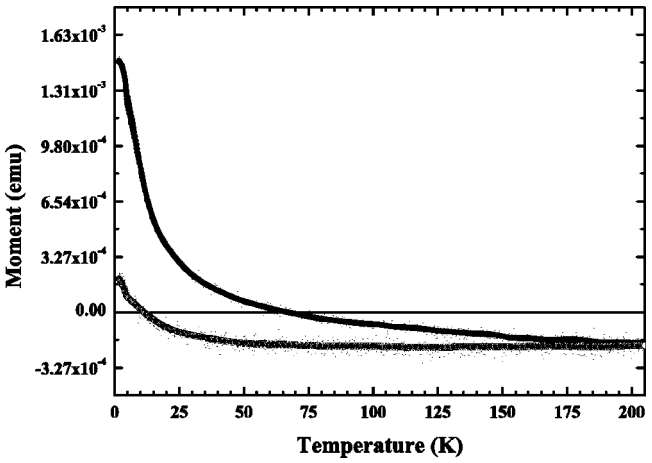

FIG. 8. Temperature dependence of the magnetic moment of the composite of carbon nanofoam and sample holder measured at $H = 30$ KOe, 15 days (upper curve) and 60 days (lower curve) after production of the sample.

in a glove box. Nevertheless, it was deemed prudent to perform the following independent experiment to determine an upper bound on the contribution of oxygen to our measurement. We filled a gelatin capsule, same as used in our measurements, with pure oxygen gas and then measured (i) the magnetic moment versus magnetic field at $T = 5$ K and (ii) the magnetic moment versus temperature at $H = 3$ T. We observed a negative total magnetic moment due to the diamagnetism of the capsule, exactly as observed for our background measurements. Any paramagnetic contribution of oxygen was too small to be observed and, hence, cannot have significantly perturbed our data.

Finally, we note another experimental observation that is incompatible with conventional FM impurities. The produced carbon nanofoam was found to exhibit a strong magnetic relaxation in time, i.e., the measured magnetic moment decreased over a period of a few days. Surprisingly, immediately after production the foam is attracted to a permanent 4 kOe $Nd_2Fe_{14}B$ magnet at room temperature, thus demonstrating the existence of a substantial permanent magnetic moment. However, the magnetization decreases sufficiently fast so that the magnet attraction effect can no longer be observed a few hours after synthesis. The filled circles in Fig. 8 shows the magnetization of the nanofoam 15 days after production and the open circles is the same measurement 60 days after production. As is evident from earlier, the magnetization exhibited by the sample relaxes to lower values as a function of time, achieving a magnetic steady state several weeks after production. We continued measuring the same sample at various intervals over the next 12 months, without any additional relaxation becoming apparent. Therefore, Figs. 3–7 represent equilibrated magnetization values.

The decrease of magnetization with time implies that some initially unpaired spins become paired. This may arise either by reaction of the spin centers with atmospheric gases such as oxygen, hydrogen, or nitrogen, or alternatively by rearrangement of localized single and double C-C bonds to eliminate pairs of spins. Whichever mechanism is operative, it is clear that the spins cannot be eliminated completely, which allows a substantial part of the initial magnetization to persist indefinitely. This behavior is consistent with the idea that some spins are sterically protected from attack by gas molecules, and also that the spins occur in finite regions of sp^2 bonding, which are isolated by "walls" of sp^3 bonding, and in which single and double bonds can be rearranged. An initial odd number of spins in such a region would leave a persistent single spin after any bonding rearrangement, provided that attack by gaseous molecules was prevented.

IV. CONCLUSIONS

The magnetic behavior exhibited by the new phase of carbon is different from the weak positive magnetization found at very low temperatures in single-walled nanohorns and activated carbon fibers, mentioned in the Sec. I. In these two cases, the occurrence of magnetism has been associated with exposed graphitic edges. Our observations point to a different origin for the magnetism in the foam. We believe that the remarkable magnetic properties of the foam, unexpected for an all-carbon material, are an intrinsic consequence of its equally remarkable nanostructure.

HRTEM shows convoluted graphite-like layers inside the nanospherulitic building blocks of the foam, the contrast being consistent with hyperbolic schwarzite curvature of the sheets.[31] This requires rings of 7 or more carbons interspersed with normal graphitic 6 rings.[35] The sheet curvature localizes unpaired spins by breaking the continuity of the delocalized π-electron clouds of graphite, and tight curvature of the sheets provides a mechanism for sterically protecting the unpaired spins which would otherwise be too chemically reactive to persist.[33]

A possible mechanism for magnetic moment generation would be a simple indirect exchange interaction through conduction electrons located on the hexagons. This, however, has to be in agreement with electrical resistivity measurements that show a semiconducting behavior with a band gap of 0.5–0.7 eV.[31] A plausible scenario would be that the magnetism of our nanofoam is an effect that actually occurs in nanosized metallic (sp^2) segments of the structure that are isolated by nonconducting (sp^3) regions, and hence, do not contribute to the overall conductivity of the sample.

The origin of magnetism in the cluster-assembled carbon nanofoam has recently been investigated theoretically using a geometry which contains hyperbolic, negatively curved, surfaces.[45] The suggested basic structural unit is a hyperbolic sheet folded into a "tetrapod" that exhibits many of the structural features observed in experiments. The core structure consists of warped sp^2 bonded carbon segments terminated by sp^3 carbon atoms at the hydrogen-passivated edges of the four extremities. The model tetrapod contains tubular domains of zero Gaussian curvature with domains of hyperbolic, saddle-like regions. The smoothed tetrapod unit is necessarily hyperbolic, of negative Gaussian curvature. The radius of curvature in this basic unit is close to 6 Å, which is consistent with the superstructure found in the diffraction pattern (though we note that this coincidence is unnecessary, as the radius is dependent only on the ring sizes in a more general hyperbolic unit).[35] The tetrapod-like building blocks

can be assembled into a rigid foam structure with a very low density that compares to the measured bulk density of $2-10\ \mathrm{mg/cm^3}$. The threefold coordinated carbon atoms in the sp^2 regions of the model tetrapod form a network of hexagons and heptagons only. These trivalent carbons are sterically protected within the system of single and double bonds imposed by the sp^3-terminated tetrapod, and occur in groups of three. The number of unpaired spins was found to be robust with respect to size and boundary shape variations within the tetrapod. However, this number depends sensitively on the bonding topology in the regions of the negative Gaussian curvature. Subclusters (tetrapods) containing 264 and 336 carbon atoms have been considered, and the predicted magnetic moment in a C_{264} tetrapod agrees well with the experimental observation.

The steric protection mechanism postulated here as well as the calculations by Park *et al.*[45] depend on a topological feature of the sp^2 carbon framework, namely the presence of rings in the framework with more than six carbon atoms.[46] That topological property induces the hyperbolic geometry of the carbon framework. The calculations of Park *et al.*[45] are for the simplest example only, containing isolated heptagons and building a four-armed "tetrapod" building node. Many distinct assemblies of such nodes are possible, leading to crystalline or random arrays, with varying amounts of strain in the network, expected to be accommodated by the introduction of rings other than hexagons and heptagons. Crystalline "polybenzene"[46] and the "random schwarzite" of Townsend *et al.*[47] and those observed in the laser-ablated nanofoams[31–33] are examples of ordered and disordered hyperbolic frameworks.

Stabilization of trivalent carbon radicals by steric protection has been known since the synthesis of triphenylmethyl by Gomberg in 1900.[48] It has recently been shown by Tomioka *et al.*[49] that even the very reactive divalent carbon radicals ("carbenes") can be stabilized to show half-lives of several minutes if the two spins can be separated onto distinct sites that are sterically protected in this way. We note that the magnetic relaxation behavior of our samples implies that there are spin centers which show differing degrees of reactivity and/or steric protection. Some unpaired spins are lost on a time scale of minutes to weeks, while others appear to be essentially permanent.

The ferromagnetism found in these complex nanoclusters occurs as a consequence of nanometer-scale conducting regions being separated by regions of a quite different electronic structure. Careful selection of laser ablation synthesis conditions may allow controlled adjustment of the properties of the product, and may allow synthesis of products with similarly unusual properties from different starting materials.

In summary, we have observed unique magnetic behavior in an all-carbon nanostructured material, whose unusual structure provides a plausible mechanism for a generation of strong magnetism. Our experimental results leads us to reject ferromagnetic impurities as the origin of the observed magnetism: the combined weight of our data, M vs H/T scaling, magnitude and temperature dependence of the moment of ferromagnetic impurities, and strong time-dependent magnetization relaxation, lead us to conclude that the observed behavior is an intrinsic property of the foam itself. The magnetic phenomena do not conform with those of conventional paramagnetism or superparamagnetism (the data do not fit the Brillouin function with $S=1/2$, and M vs H/T curves do not collapse onto one another). We have observed small hysteresis and remnant magnetization in the $M(H)$ curve of our foam which are usually observed in organic ferromagnets[50] and, hence, do not exclude the case of weak soft ferromagnetism. Nevertheless, we have no clear signs of an ordering temperature.

This new form of carbon clearly warrants further theoretical and experimental investigations.

ACKNOWLEDGMENTS

The authors are grateful to Professor D. Tománek of Michigan State University, for many encouraging discussions, followed by exchange of, in total, 272 e-mail messages. E.G.G. acknowledges the assistance of the Australian Research Council under the ARC Centres of Excellence program through the Centre for Ultrahigh bandwidth Devices for Optical Systems (CUDOS).

*Authors to whom correspondence should be addressed.
†Electronic address: avr111@rsphy1.anu.edu.au
‡Electronic address: giapintz@iesl.forth.gr

[1] F. Laves and Y. Baskin, Z. Kristallogr. **107**, 337 (1956).
[2] C. Frondel and U. B. Martin, Nature (London) **214**, 587 (1967).
[3] A. El Goresy and G. Donnay, Science **161**, 363 (1968).
[4] C. T. Pillinger, Philos. Trans. R. Soc. London, Ser. A **343**, 73 (1993).
[5] K. Yamada, Y. Tanabe, and A. B. Sawaoka, Philos. Mag. A **80**, 1811 (2000).
[6] J. B. Donnet, E. Fousson, M. Samirant, T. K. Wang, M. Pontier-Johnson, and A. Eckhardt, C.R. Acad. Sci., Ser. IIc: Chim **3**, 359 (2000).
[7] V. V. Milyavskiy, T. I. Borodina, A. Z. Zhuk, and V. E. Fortov, Mol. Mater. **13**, 361 (2000).
[8] R. B. Heimann, Diamond Relat. Mater. **3**, 1151 (1994).
[9] Yu. P. Kudryatsev, R. B. Heimann, and S. E. Evsyukov, J. Mater. Sci. **31**, 5557 (1996).
[10] P. Fraundorf and M. Wackenhut, Astrophys. J. **578**, L153 (2002).
[11] H. W. Kroto, J. R. Heath, S. C. O'Brien, R. F. Curl, and R. E. Smalley, Nature (London) **318**, 162 (1985).
[12] W. Krätschmer, L. D. Lamb, K. Fostiropoulos, and D. R. Huffmann, Nature (London) **347**, 354 (1990).
[13] S. Iijima, Nature (London) **354**, 56 (1991).
[14] S. Iijima and T. Ichihashi, Nature (London) **363**, 603 (1993).
[15] C. N. R. Rao, R. Seshadri, A. Govindaraj, and R. Sen, Mater. Sci. Eng., R. **15**, 209 (1995).
[16] T. L. Makarova, B. Sundqvist, R. Höhne, P. Esquinazi, Y. Kopelevich, P. Scharff, V. A. Davydov, L. S. Kashevarova, and A. V. Rakhmanina, Nature (London) **413**, 716 (2001).

[17] J-C. Charlier, P. Lambin, and T. W. Ebbesen, Phys. Rev. B **54**, R8377 (1996).
[18] R. Saito, M. Fujita, G. Dresselhaus, and M. S. Dresselhaus, Phys. Rev. B **46**, 1804 (1992).
[19] L. C. Venema, V. Meunier, Ph. Lambin, and C. Dekker, Phys. Rev. B **61**, 2991 (2000).
[20] R. H. Baughman, A. A. Zakhidov, and W. A. de Heer, Science **297**, 787 (2002).
[21] Y. Shibayama, H. Sato, T. Enoki, and M. Enda, Phys. Rev. Lett. **84**, 1744 (2000).
[22] S. Bandow, F. Kokai, K. Takahashi, M. Yudasaka, and S. Iijima, Appl. Phys. A: Mater. Sci. Process. **A73**, 281 (2001).
[23] L. Liu, G. Y. Guo, C. S. Jayanthi, and S. Y. Wu, Phys. Rev. Lett. **88**, 217206 (2002).
[24] K. Tanaka, M. Kobashi, H. Sanekata, A. Takata, T. Yamabe, S. Mizogami, and K. Kawabata, J. Appl. Phys. **71**, 836 (1992).
[25] K. Murata and H. Ushijima, J. Appl. Phys. **79**, 978 (1996).
[26] A. A. Ovchinnikov and V. N. Spector, Synth. Met. **27**, 615 (1988).
[27] K. Murata, H. Ueda, and K. Kawaguchi, Synth. Met. **44**, 357 (1991).
[28] K. Murata, H. Ushijima, H. Ueda, and K. Kawaguchi, J. Chem. Soc., Chem. Commun. **18**, 1265 (1991).
[29] P. Esquinazi, D. Spemann, R. Höhne, A. Setzer, K.-H. Han, and T. Butz, Phys. Rev. Lett. **91**, 227201 (2003).
[30] K. Kusakabe and M. Maruyama, Phys. Rev. B **67**, 092406 (2003).
[31] A. V. Rode, S. T. Hyde, E. G. Gamaly, R. G. Elliman, D. R. McKenzie, and S. Bulcock, Appl. Phys. A: Mater. Sci. Process. **A69**, S755 (1999).
[32] A. V. Rode, E. G. Gamaly, and B. Luther-Davies, Appl. Phys. A: Mater. Sci. Process. **A70**, 135 (2000).
[33] A. V. Rode, R. G. Elliman, E. G. Gamaly, A. I. Veinger, A. G. Christy, S. T. Hyde, and B. Luther-Davies, Appl. Surf. Sci. **197–198**, 644 (2002).
[34] D. Vanderbilt and J. Tersoff, Phys. Rev. Lett. **68**, 511 (1991).
[35] S. T. Hyde and M. O'Keeffe, Philos. Trans. R. Soc. London, Ser. A **354**, 1999 (1996).
[36] A. L. Mackay and H. Terrones, Nature (London) **352**, 762 (1991).
[37] S. T. Hyde, in *Defects and Processes in the Solid State*, edited by J. D. Fitz Gerald and J. N. Boland (Elsevier, Amsterdam, 1993).
[38] E. G. Gamaly, A. V. Rode, and B. Luther-Davies, Appl. Phys. A: Mater. Sci. Process. **A69**, S121 (1999).
[39] M. S. Dresselhaus, Annu. Rev. Mater. Sci. **27**, 1 (1997).
[40] A. W. P. Fung, Z. H. Wang, K. Lu, M. S. Dresselhaus, and R. W. Pekala, J. Mater. Res. **8**, 1875 (1993).
[41] A. W. P. Fung, Z. H. Wang, M. S. Dresselhaus, G. Dresselhaus, R. W. Pekala, and M. Endo, Phys. Rev. B **49**, 17 325 (1994).
[42] D. R. McKenzie, Rep. Prog. Phys. **59**, 1611 (1996).
[43] C. Kittel, *Introduction to Solid State Physics*, 4th ed. (Wiley, New York, 1971).
[44] F. Hellman, M. Q. Tran, A. E. Gebala, E. M. Wilcox, and R. C. Dynes, Phys. Rev. Lett. **77**, 4652 (1996).
[45] N. Park, M. Yoon, S. Berber, J. Ihm, E. Osawa, and D. Tomanek, Phys. Rev. Lett. **91**, 237204 (2003).
[46] M. O'Keeffe, G. B. Adams, and O. F. Sankey, Phys. Rev. Lett. **68**, 2325 (1992).
[47] S. J. Townsend, T. J. Lenosky, D. A. Muller, C. S. Nichols, and V. Elser, Phys. Rev. Lett. **69**, 921 (1992).
[48] M. Gomberg, J. Am. Chem. Soc. **22**, 757 (1900).
[49] H. Tomioka, E. Iwamoto, H. Itakura, and K. Hirai, Nature (London) **412**, 626 (2001).
[50] A. Mrzel, A. Omerzu, P. Umek, D. Mihailovic, Z. Jaglicic, and Z. Trontelj, Chem. Phys. Lett. **298**, 329 (1998).